

An XUV Source using a Femtosecond Enhancement Cavity for Photoemission Spectroscopy

Arthur K. Mills^a, Sergey Zhdanovich^a, Alex Sheyerman^a, Giorgio Levy^{a,b},
Andrea Damascelli^{a,b}, and David J. Jones^a

^aDepartment of Physics and Astronomy, ^bQuantum Matter Institute,
Vancouver, British Columbia V6T 1Z1, Canada

ABSTRACT

Recent development of extreme ultraviolet (XUV) sources based on high harmonic generation (HHG) in femtosecond enhancement cavities (fsEC) has enabled generation of high photon flux ($\sim 10^{13}$ - 10^{14} photons/sec) in the XUV, at high repetition rates (> 50 MHz) and spanning the spectral region from 40 nm - 120 nm. Here we demonstrate the potential offered by this approach for angle-resolved photoemission spectroscopy by measuring the photoemission spectrum of Au using 8.3 and 25 eV photons with excellent resolution at rapid data rates.

Keywords: Femtosecond Enhancement Cavity, High Harmonic Generation, Photoemission Spectroscopy, Femtosecond Fiber Lasers

1. INTRODUCTION

Using amplified femtosecond (fs) pulses and high harmonic generation (HHG), laser-based sources have generated spatially and temporally coherent radiation from the vacuum/extreme ultra-violet (VUV/XUV) down to the soft X-ray region, leading to several advances in electron imaging¹ and attosecond physics^{2,3} among other topics. Despite these successes such sources are not ideal for photoemission spectroscopy⁴ where the low repetition rate (~ 1 - 500 kHz) causes a variety of problems including prohibitively low data rates and high peak XUV power, the latter leading to parasitic space charge effects and material damage/modification as well as other issues.

By employing a femtosecond enhancement cavity (fsEC) together with intra-cavity HHG, a new type of VUV/XUV femtosecond source has recently emerged^{5,6} that addresses the shortcomings of current laser-based, single-pass HHG sources when used for photoemission spectroscopy. In fsECs, the phase evolution of successive pulses incident on the cavity is controlled such that they phase-coherently add with the existing pulse stored in the cavity and significant enhancement of intracavity pulse energy can be obtained (> 100 uJ) at the full repetition rate (~ 50 MHz) of the mode-locked oscillator. A gas target is placed inside the cavity and the high energy, high repetition rate pulse train drives the HHG process to produce XUV pulses with the same repetition rate.

These fsEC sources with a table-top footprint can offer photon-fluxes $> 10^{13}$ photons/s to 32 eV photon energies [4] and when pushed they can deliver photons energies out to 100 eV at albeit lower flux.⁷ And perhaps most intriguingly they can occupy a sweet spot of short enough pulses (~ 100 fs) for time-resolved photoemission studies while still maintaining low enough energy resolution (~ 30 meV), acceptable photon fluxes, high repetition rates (> 10 MHz for adequate data acquisition rates) and generation of high photon energies.

Motivated by these attributes we have been pursuing time-resolved, angle-resolved photoemission spectroscopy (tr-ARPES) using such fsEC XUV sources. The characterization of the source's performance and resolution (by evaluating the Fermi energy of an evaporated gold sample) has confirmed its significant promise. In this work we report our progress toward employing a fsEC XUV source for tr-APRES studies of correlated electron systems to study topological states and time dynamics of quasi-particles among other topics.

Further author information: (Send correspondence to D.J.J.)
E-mail: djones@physics.ubc.ca, Telephone: +1 604 822 2894

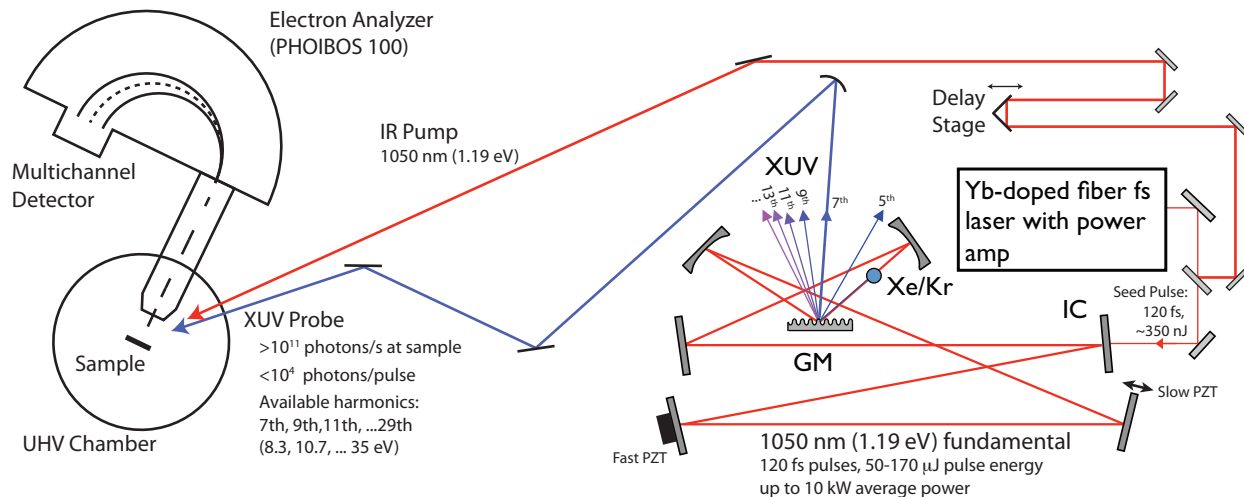


Figure 1. Schematic of the experimental apparatus. A Yb-doped fs fiber laser with power amplifier supplies seed pulses which are coupled to the fsEC through the 0.8% input coupler (IC), where pulses in excess of 150 μJ are obtained inside the cavity. The round trip time of pulses in the fsEC is stabilized to the seed laser repetition rate using fast and slow PZT actuators. HHG is performed at the tight focus within the fsEC. The resulting harmonics are coupled out of the fsEC with a diffraction grating mirror (GM). The desired harmonic is steered to the photoemission ultrahigh vacuum (UHV) chamber through several stages of differential pumping (not shown) with three boron-carbide coated spherical mirrors. Photoelectrons are then analyzed with the Phoibos 100 analyzer with channeltron detector.

2. EXPERIMENTAL APPARATUS

The fsEC XUV source consists of two components; the passive enhancement cavity itself, and the laser source used to seed the enhancement cavity where the high harmonic generation is performed. The laser source is based on a ytterbium-doped fiber (YDF) laser oscillator with two YDF amplifiers, with operating wavelengths at $1.050 \mu\text{m}$. The output of the final power amplifier stage is used as the seed for the fsEC. High harmonic generation is performed in the tight focus of the fsEC, and the resulting VUV and XUV light is coupled out of the cavity with an intracavity diffraction grating and directed to the ultraviolet photoemission chamber. A schematic representation of the system, with a summary of performance specifications, is shown in Fig. 1.

2.1 Amplified YDF Laser Source

The laser source seeding the fsEC system is based on a home-built YDF ring oscillator that is mode-locked using nonlinear polarization evolution.⁸ The laser has a tuneable bandwidth and central wavelength, but is typically operated with a bandwidth of about 12 nm, a central wavelength near 1050 nm (1.19 eV), and an average power of about 30 mW and a pulse repetition rate of 60 MHz. The oscillator has a pair of intracavity transmission gratings (in a double-pass configuration) that enables us to tune the dispersion of the cavity and control the mode-locking regime used. To limit the spectral bandwidth, we run the oscillator with a small amount of anomalous dispersion, where the spectral shape has a nearly sech profile. This operating point is a trade-off between spectral bandwidth and noise properties of the oscillator. The bandwidth decreases with increasing anomalous dispersion, and intensity noise and carrier-envelope offset noise levels are minimized close to zero dispersion (the latter measured indirectly through the fsEC intracavity intensity). Our experience with this laser is consistent with the results of a detailed study of the intensity and offset frequency noise of this type of YDF oscillator.⁹

The positively chirped pulse train emerging from the output of the oscillator is passed directly into a single mode YDF preamplifier, which results in further stretching due to the normal dispersion of the fiber. The nearly 300 mW average power output of the preamplifier is then directed into the photonic crystal fiber (PCF) power amplifier made up of 3 m of Yb-doped PCF pumped with up to 80 W at 976 nm. The complete amplified YDF laser system is shown in Fig. 2.

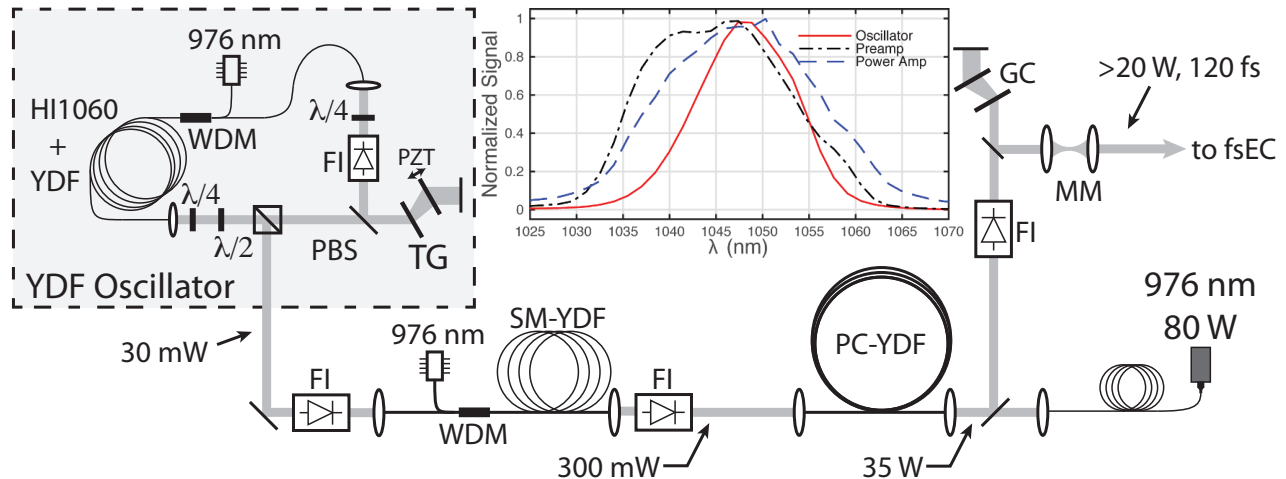


Figure 2. Schematic of the Amplified YDF laser source. The laser source is a YDF oscillator comprised of HI1060 single mode fiber, single mode YDF, a free-space section to produce a repetition rate of 60 MHz. The intracavity transmission gratings (TG) allow tuning of the net dispersion of the cavity, one of which is on a PZT actuated stage that allows for slow control of the carrier-envelope offset frequency. Mode-locking is achieved through nonlinear polarization evolution, which acts as a saturable absorber when the wave plates ($\lambda/4$, $\lambda/2$) are set in a suitable configuration. The laser is pumped with a single mode 976 nm diode coupled into the oscillator through an intracavity wavelength division multiplexer (WDM). The preamplifier is a single mode YDF (SM-YDF), and the power amplifier is a photonic crystal YDF (PC-YDF), pumped with up to 80 W at 976 nm. The pulses emerging from the power amplifier are compressed down to 120 fs duration with a transmission grating compressor (GC), and after the mode-matching telescope (MM) over 20 W of average power is available to seed the fsEC.

We do observe nonlinear behavior in the PCF amplifier, in that at high pump power we have seen some broadening of the spectrum. We have not characterized these properties extensively, except to note that even with a compressed pulse launched into the PCF, the enhancement and noise properties of the stabilized fsEC are not degraded when the PCF amplifier is operating in this nonlinear regime. Moreover as shown by the inset in Fig. 2 the power amplified pulse does not suffer any gain narrowing. This provides a relatively simple alternative to systems that employ linear amplification.¹⁰ The output of the power amp is compressed with a transmission grating compressor, after which up to 25 W (or ~ 400 nJ) is available as a seed to the fsEC. The compressed pulse width is typically about 120 fs (intensity autocorrelation), and we observe only a small amount of structure in the wings of the pulse. This laser system has proven a nearly ideal seed source (in terms of pulse width and peak power) for the fsEC when utilized for tr-ARPES as pulses much below 100 fs are too detrimental for ARPES resolution.

2.2 Femtosecond Enhancement Cavity

The fsEC is comprised of seven mirrors in a ring configuration with a 5 m round trip length, as shown at the right of Fig. 1. A focus with a waist radius of $20 \mu\text{m}$ is formed in between two 15 cm ROC curved mirrors, and the finesse of the cavity is reduced using a 0.8% input coupler, which yields an enhancement factor of several hundred times. The cavity length is stabilized with a fast PZT actuator to compensate high frequency perturbations and a slow, long range PZT to correct for slow drift in the cavity length. The carrier-envelope offset frequency of the oscillator is matched to that of the fsEC, which is actuated with a slow PZT that changes the diffraction grating separation in the oscillator. We find that only slow correction of the offset frequency is needed to maintain a good intensity stability in the fsEC as its finesse is not too high. We achieve good spatial mode matching to the cavity ($> 85\%$), and we measure intracavity average powers in excess of 5 kW. When the cavity is stabilized, a short-term intensity stability (intracavity) of less than 0.25%, with 1% drift over longer periods (many hours), is possible. The day-to-day fsEC performance is also very stable: once operational, the system has been run for several months without the need to realign the cavity mirrors.

High harmonic generation is performed at the tight focus of the fsEC. We have used xenon (Xe) and krypton (Kr) for the gas target, which is injected just above the cavity focus through a 150 μm quartz nozzle placed as close to the fsEC beam as possible without causing significant loss or heating of the nozzle. The harmonics are coupled out of the fsEC with an intracavity diffraction grating etched into the outermost layer of a mirror placed in the fsEC immediately after the focus (labelled GM in Fig. 1). The grating has a 200 nm period and is etched into the top layer of the dielectric stack, which results in a diffraction efficiency of a few percent per harmonic. We image a phosphor-coated plate to detect the harmonics coupled out of the fsEC, and with Xe we have observed up to the 23rd harmonic (27.4 eV). Using an uncalibrated aluminum filtered XUV photodiode (IRD Inc), we have measured several microwatt level power for the 15th harmonic (at 17.8 eV) coupled out of the fsEC.

The plasma generated at the focus of the fsEC poses a challenge for fsEC XUV generation in that the plasma causes a phase shift for the near-infrared fundamental pulse circulating in the cavity. In addition to dynamic phase shifts that limit the pulse enhancement on the femtosecond timescale, the linear plasma phase shift combined with intensity fluctuations in the seed source can drive oscillations of the intracavity intensity as the plasma grows and collapses very rapidly in response to intensity fluctuations.^{6,11} With Xe, this limitation is quite severe at relatively modest intracavity average power due to its lower ionization potential. A successful strategy to reduce the ionization-related clamping of XUV generation is to reduce the pulse width of the fsEC pulses.⁷ In our case, the reduced energy resolution with this approach is not desirable. When we use Kr gas at the same intracavity average power where the XUV generation clamped with Xe, we see a substantially reduced plasma and harmonic flux, as expected. We do not see any effects of plasma instability inside the cavity even at the maximum output of our power amplifier system. At this level, we measure nearly the same power for the 15th harmonic that we did in Xe, and we observe up to the 29th harmonic (34.5 eV). Further gains may still be achieved with Kr by increasing the finesse of the fsEC, however the sensitivity to phase fluctuations will eventually limit XUV produced.

The XUV flux from the fsEC is also quite stable with short term (a few minutes) intensity stability on the order of 2-3%, and longer term stability of less than 10% (in part due to imperfect gas target pressure regulation). The fsEC XUV source also produces an output beam with good pointing stability. The alignment of the XUV beams into the photoemission experiment (> 1 m away) is difficult to detect over periods of several days.

An important factor in maintaining a long operating time of the fsEC XUV source has been to mitigate hydrocarbon build-up on the optics that are exposed to VUV/XUV light. So far, this has not been possible through the use of UHV-compatible vacuum practices alone. In addition, what has proven effective is steady in-situ cleaning of the exposed mirrors with ozone (with a concentration of a few percent in an oxygen gas flow) during XUV production. In our system, we use small glass nozzles to efficiently direct the flow of ozone/oxygen onto the mirror surfaces where they are exposed to the VUV/XUV light. We have not thoroughly tested the flow rate required to keep the mirrors clean, rather we use a gas flow rate that doesn't significantly load our vacuum system turbo pump or dramatically raise the pressure in the chamber when Xe/Kr gas is flowing (*i.e.* $\sim 10^{-3}$ mbar with our pumping geometry). This method has eliminated hydrocarbon build-up related degradation of the fsEC mirrors, namely the XUV diffraction grating mirror and the curved mirror immediately after the grating mirror. We have also observed slow build-up of hydrocarbons on the next mirror in the path of the fsEC, which is also exposed to UV light, and we clean this mirror every few months in a laboratory oxygen plasma cleaner. A future cavity upgrade will include an in situ ozone/oxygen nozzle on this mirror as well.

2.3 Ultraviolet Photoemission Spectrometer

The photoemission spectroscopy was carried out in an ultraviolet photoemission spectrometer (UPS) built around a Specs Phoibos 100 electron analyzer with channeltron multichannel detector, with a sample load-lock chamber and gold evaporator. This analyzer system was originally intended for use as an X-ray photoelectron spectrometer, and as such, the magnetic shielding was not ideal for low energy electron spectroscopy. However, this system provided a sufficient proof of principle test chamber to test the viability XUV source for photoemission spectroscopy. We are currently upgrading the system to a system with a much higher resolution analyzer for ARPES and sample chamber that is properly shielded from magnetic fields.

3. EXPERIMENTAL RESULTS

In Fig. 3 we show UPS spectra for room temperature gold excited with 8.3 and 25 eV photon energies. In this experiment, the 7th harmonic (8.3 eV) was directed to the UPS experiment. The 25 eV signal is due to 3rd order diffraction of the 21st harmonic that co-propagates with the 1st order diffraction of the 7th harmonic. For the laser intensity used in this experiment, with Xe gas, the 21st harmonic was above the HHG cut-off for the plateau harmonics, meaning that the photon flux generated for the 21st harmonic is substantially reduced from that of the lower harmonics. Further, the 3rd order diffraction from the grating output coupler is lower in power than the first order diffraction. That the photoemission signal is observable at this collection time (1 sec) is largely due to the much higher photoemission cross section at 25 eV compared to 8.3 eV. Nevertheless, a Fermi edge (albeit quite noisy) can be seen at approximately 21 eV kinetic energy.

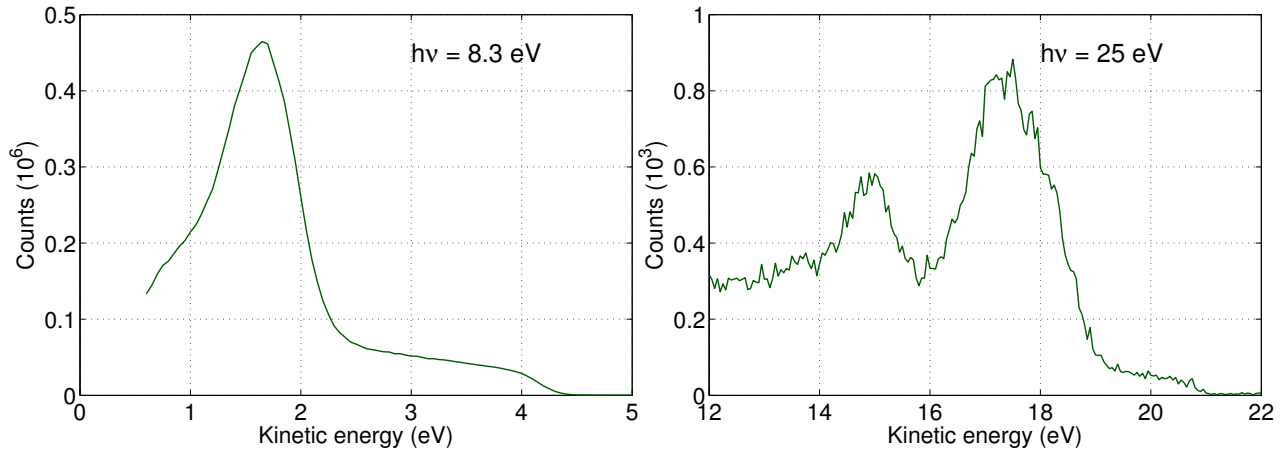


Figure 3. Room temperature gold photoemission spectra for 8.3 eV (left) and 25 eV (right) photons. Photoelectron counts represents signal in 1 second intervals.

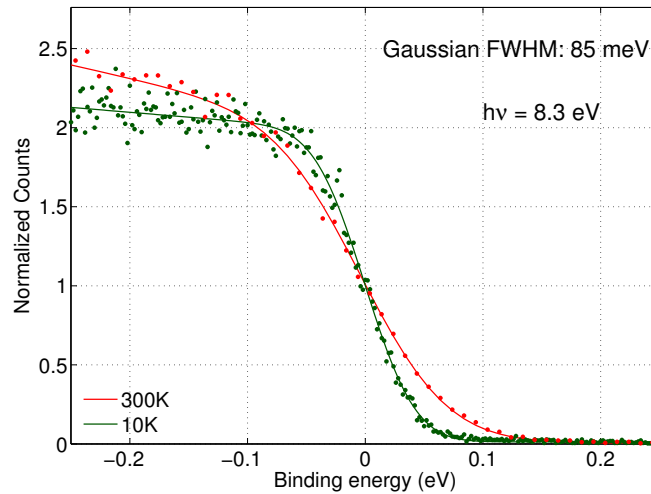


Figure 4. Gold Fermi edge signal at 300 K and 10 K. Theoretical fit to the data indicates a Gaussian FWHM resolution of 85 meV, which is believed to be dominated by the resolution of the analyzer in this dataset.

4. CONCLUSION

We have built a femtosecond enhancement cavity based XUV source for performing photoemission spectroscopy of quantum matter systems. For our seed pulse duration of about 120 fs, a photon-flux on the microwatt-level up to the 23rd harmonic (or 27.4 eV photon energy) can be generated by the system with Xe as the target gas. This power level is limited by plasma induced bi-stabilities inside the cavity. With Kr as the target gas and the full laser power available in our system, a similar power performance level is achieved while extending the achievable photon energy to 34.4 eV (or the 29th harmonic).

We presented initial results of gold photoemission using this source with 8.3 and 25 eV photons. The 85 meV resolution achieved in these measurements was largely determined by the spectrometer used. Future work will involve replacing the UPS spectrometer with a higher resolution angle-resolved photoemission spectrometer and implementing a near-infrared pump source to perform time-resolved ARPES measurements. With these improvements we will be able to test the predictions of time resolution at the 100-200 fs level for time resolved measurements with an energy resolution in the 20-30 meV range. Such a source should prove very useful in studying quantum matter systems.

ACKNOWLEDGMENTS

The authors gratefully acknowledge the contributions of TJ Hammond and Riccardo Comin and the financial support by Natural Science and Engineering Research Council (NSERC), Canadian Foundation for Innovation and British Columbia Knowledge Development Fund.

REFERENCES

1. A. Baltuska, T. Udem, M. Uiberacker, M. Hentschel, E. Goulielmakis, C. Gohle, R. Holzwarth, V. S. Yakovlev, A. Scrinzi, T. W. Hänsch, and F. Krausz, "Attosecond control of electronic processes by intense light fields.," *Nature* **421**(6923), pp. 611–615, 2003.
2. E. Goulielmakis, Z.-H. Loh, A. Wirth, R. Santra, N. Rohringer, V. S. Yakovlev, S. Zherebtsov, T. Pfeifer, A. M. Azzeer, M. F. Kling, S. R. Leone, and F. Krausz, "Real-time observation of valence electron motion.," *Nature* **466**(7307), pp. 739–743, 2010.
3. M. Uiberacker, T. Uphues, M. Schultze, A. J. Verhoef, V. Yakovlev, M. F. Kling, J. Rauschenberger, N. M. Kabachnik, H. Schröder, M. Lezius, K. L. Kompa, H.-G. Müller, M. J. J. Vrakking, S. Hendel, U. Kleineberg, U. Heinzmann, M. Drescher, and F. Krausz, "Attosecond real-time observation of electron tunnelling in atoms.," *Nature* **446**, pp. 627–32, May 2007.
4. A. Damascelli, Z. Hussain, and Z. Shen, "Angle-resolved photoemission studies of the cuprate superconductors," *Reviews of Modern Physics* **75**, p. 473, Apr. 2003.
5. A. K. Mills, T. J. Hammond, M. H. C. Lam, and D. J. Jones, "XUV frequency combs via femtosecond enhancement cavities," *Journal of Physics B: Atomic, Molecular and Optical Physics* **45**, p. 142001, July 2012.
6. D. C. Yost, A. Cingöz, T. K. Allison, A. Ruehl, M. E. Fermann, I. Hartl, and J. Ye, "Power optimization of XUV frequency combs for spectroscopy applications [Invited]," *Optics Express* **19**, pp. 23483–93, Dec. 2011.
7. I. Pupeza, S. Holzberger, T. Eidam, H. Carstens, D. Esser, J. Weitenberg, P. Russbüldt, J. Rauschenberger, J. Limpert, T. Udem, A. Tünnermann, T. Hänsch, A. Apolonski, F. Krausz, and E. Fill, "Compact high-repetition-rate source of coherent 100 eV radiation," *Nat Photon* **7**(8), p. 608, 2013.
8. H. Lim, F. O. Ilday, and F. W. Wise, "Generation of 2-nJ pulses from a femtosecond ytterbium fiber laser," *Optics Letters* **28**, p. 660, Apr. 2003.
9. L. Nugent-Glandorf, T. A. Johnson, Y. Kobayashi, and S. A. Diddams, "Impact of dispersion on amplitude and frequency noise in a Yb-fiber laser comb.," *Optics letters* **36**(9), pp. 1578–1580, 2011.
10. A. Ruehl, A. Marcinkevicius, M. E. Fermann, and I. Hartl, "80 W, 120 fs Yb-fiber frequency comb," *Optics Letters* **35**, p. 3015, Sept. 2010.
11. D. R. Carlson, J. Lee, J. Mongelli, E. M. Wright, and R. J. Jones, "Intracavity ionization and pulse formation in femtosecond enhancement cavities," *Optics Letters* **36**, pp. 2991–3, Aug. 2011.